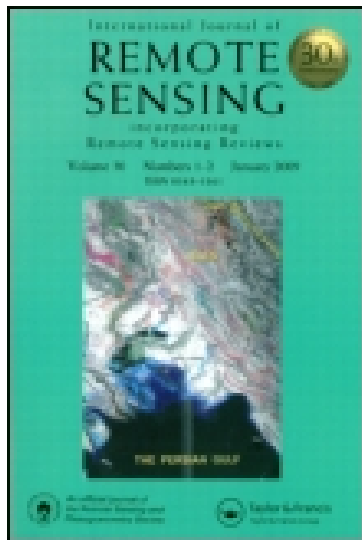


This article was downloaded by: [University of Victoria]

On: 12 June 2015, At: 08:38

Publisher: Taylor & Francis

Informa Ltd Registered in England and Wales Registered Number: 1072954 Registered office: Mortimer House, 37-41 Mortimer Street, London W1T 3JH, UK



[Click for updates](#)

International Journal of Remote Sensing

Publication details, including instructions for authors and subscription information:

<http://www.tandfonline.com/loi/tres20>

Estimating daily maximum air temperature from MODIS in British Columbia, Canada

Yongming Xu^{ab}, Anders Knudby^c & Hung Chak Ho^c

^a School of Remote Sensing, Nanjing University of Information Science & Technology, Nanjing 210044, PR China

^b Beijing Institute of Urban Meteorology, China Meteorological Administration, Beijing 100089, PR China

^c Department of Geography, Simon Fraser University, Burnaby, British Columbia, Canada V5A 1S6

Published online: 04 Dec 2014.

To cite this article: Yongming Xu, Anders Knudby & Hung Chak Ho (2014) Estimating daily maximum air temperature from MODIS in British Columbia, Canada, International Journal of Remote Sensing, 35:24, 8108-8121, DOI: [10.1080/01431161.2014.978957](https://doi.org/10.1080/01431161.2014.978957)

To link to this article: <http://dx.doi.org/10.1080/01431161.2014.978957>

PLEASE SCROLL DOWN FOR ARTICLE

Taylor & Francis makes every effort to ensure the accuracy of all the information (the "Content") contained in the publications on our platform. However, Taylor & Francis, our agents, and our licensors make no representations or warranties whatsoever as to the accuracy, completeness, or suitability for any purpose of the Content. Any opinions and views expressed in this publication are the opinions and views of the authors, and are not the views of or endorsed by Taylor & Francis. The accuracy of the Content should not be relied upon and should be independently verified with primary sources of information. Taylor and Francis shall not be liable for any losses, actions, claims, proceedings, demands, costs, expenses, damages, and other liabilities whatsoever or howsoever caused arising directly or indirectly in connection with, in relation to or arising out of the use of the Content.

This article may be used for research, teaching, and private study purposes. Any substantial or systematic reproduction, redistribution, reselling, loan, sub-licensing, systematic supply, or distribution in any form to anyone is expressly forbidden. Terms &

Conditions of access and use can be found at <http://www.tandfonline.com/page/terms-and-conditions>

Estimating daily maximum air temperature from MODIS in British Columbia, Canada

Yongming Xu^{a,b,*}, Anders Knudby^c, and Hung Chak Ho^c

^aSchool of Remote Sensing, Nanjing University of Information Science & Technology, Nanjing 210044, PR China; ^bBeijing Institute of Urban Meteorology, China Meteorological Administration, Beijing 100089, PR China; ^cDepartment of Geography, Simon Fraser University, Burnaby, British Columbia, Canada V5A 1S6

(Received 23 August 2014; accepted 20 September 2014)

Air temperature (T_a) is an important climatological variable for forest research and management. Due to the low density and uneven distribution of weather stations, traditional ground-based observations cannot accurately capture the spatial distribution of T_a , especially in mountainous areas with complex terrain and high local variability. In this paper, the daily maximum T_a in British Columbia, Canada was estimated by satellite remote sensing. Aqua MODIS (Moderate Resolution Imaging Spectroradiometer) data and meteorological data for the summer period (June to August) from 2003 to 2012 were collected to estimate T_a . Nine environmental variables (land surface temperature (LST), normalized difference vegetation index (NDVI), modified normalized difference water index (MNDWI), latitude, longitude, distance to ocean, altitude, albedo, and solar radiation) were selected as predictors. Analysis of the relationship between observed T_a and spatially averaged remotely sensed LST indicated that 7×7 pixel size was the optimal window size for statistical models estimating T_a from MODIS data. Two statistical methods (linear regression and random forest) were used to estimate maximum T_a , and their performances were validated with station-by-station cross-validation. Results indicated that the random forest model achieved better accuracy (mean absolute error, MAE = 2.02°C, R^2 = 0.74) than the linear regression model (MAE = 2.41°C, R^2 = 0.64). Based on the random forest model at 7×7 pixel size, daily maximum T_a at a resolution of 1 km in British Columbia in the summer of 2003–2012 was derived, and the spatial distribution of summer T_a in this area was discussed. The satisfactory results suggest that this modelling approach is appropriate for estimating air temperature in mountainous regions with complex terrain.

1. Introduction

Near-surface air temperature, also referred to as air temperature, is usually measured at meteorological shelter height (about 2 m above ground). Air temperature is an important meteorological variable that influences forest ecosystems. It plays a critical role in vegetation distributions, phenology, and growth (Benavides et al. 2007; Stahl et al. 2006). The maximum daytime temperature also shows significant relationship with the occurrence of wildfire on hot and sunny days (Aldersley, Murray, and Cornell 2011; Litschert, Brown, and Theobald 2012). Therefore, detailed knowledge of the spatial variability of air temperature is of interest for forest research and management.

*Corresponding author. Email: xym30@263.net

Traditionally, T_a is measured by weather stations, which provide observed data at discrete locations. However, weather stations are usually sparsely distributed in mountainous regions, especially in high-elevation areas, and thus may not optimally represent all environments (Rolland 2003). Given the large spatial heterogeneity of T_a in complex terrain (Holden et al. 2011), it is difficult to accurately characterize the distribution of T_a over mountainous areas (Carrega 1995). Different interpolation methods have been used to generate spatially continuous T_a from point station measurements (Benavides et al. 2007; Dodson and Marks 1997; Duhan et al. 2013; Kurtzman and Kadmon 1999; Stahl et al. 2006). However, the performance of interpolation methods is highly dependent on the spatial density and distribution of weather stations (Chan and Paelinckx 2008; Vogt, Viau, and Paquet 1997), which is not considered satisfactory in mountainous areas.

Satellite remote sensing provides the ability to extract spatially continuous information on near-surface environmental conditions, which can provide more spatial detail than ground-based measurements (Czajkowski et al. 1997; Kim and Han 2013). Over the past 20 years, various methods have been proposed to derive T_a using remote-sensing data. Most of the methods estimate T_a based on remotely sensed land surface temperature (LST), which greatly influences T_a , particularly on clear-sky days (Benali et al. 2012). Generally, these methods can be divided into three groups: the temperature–vegetation index (TVX) approach (Czajkowski et al. 1997; Goward et al. 1994; Nieto et al. 2011; Prihodko and Goward 1997; Wloczyk et al. 2011; Zhu, Lü, and Jia 2013), statistical approaches (Benali et al. 2012; Florio et al. 2004; Jang, Viau, and Anctil 2004; Kim and Han 2013; Xu, Qin, and Shen 2012; Zhang et al. 2011), and surface energy balance approaches (Pape and Löffler 2004; Sun et al. 2005). The TVX method is based on the hypothesis that T_a within an infinitely thick canopy is equal to the canopy surface temperature (Prihodko and Goward 1997). In this method, a parameter, maximum normalized difference vegetation index ($NDVI_{max}$), is adopted to represent a fully vegetated canopy. According to the negative relationship between surface temperature and NDVI in a relatively small window assuming uniform atmospheric conditions, the LST value at $NDVI_{max}$ can be calculated and set equal to T_a . Statistical approaches usually estimate T_a by combining LST and other variables, such as NDVI, elevation, latitude, and longitude. Regression is the most frequently used statistical method to estimate T_a , ranging from multiple linear regression to more complex models such as artificial neural networks. Surface energy balance approaches are based on the physical principle that the sum of the sensible heat flux, latent heat flux, and soil heat flux is equal to the net radiation. The latent heat flux and sensible heat flux can be expressed as functions of the difference between T_a and LST. Therefore the difference between T_a and LST can be calculated according to the surface energy balance equation, which is a complex function of solar radiation, wind speed, soil moisture, surface roughness, surface albedo, and other variables. Based on the quantitative relationship between T_a and the remotely sensed LST, T_a can be derived.

The objective of this study was to estimate the maximum daily air temperature with high spatial resolution in British Columbia, Canada from Moderate Resolution Imaging Spectroradiometer (MODIS) data by a proper statistical method. Specifically, the spatial scale effects of the relationship between T_a and LST were first analysed to determine the best window size to retrieve T_a in the study area. Then linear regression and random forest models were developed to estimate T_a , and their accuracy was evaluated by comparison with observed air temperature data from weather stations.

2. Study area and data set

2.1. Study area

The province of British Columbia is situated in western Canada, from 48.31° N to 60.00° N and 114.07° W to 139.04° W, and has a total land area of 944,735 km². This region is characterized by mountainous terrain, except for the northeastern plains. Forest is the major land-cover type, covering almost 60% of the province (B.C. Ministry of Forests, Mines and Lands 2010). Most of the forest (83%) is dominated by conifers.

Influenced by the Pacific Ocean, mountainous topography, and the ~12° latitude range, British Columbia has a number of different climatic zones. Generally, coastal British Columbia has a mild, rainy oceanic climate, and the interior has a semi-arid climate. During the summer, the influence of the North Pacific high-pressure system brings hot and dry weather to most regions in British Columbia, increasing the risk of wildfire (Pike et al. 2010). According to the historical fire data of 1950–2012 provided by DataBC Geographic Services, approximately 70% of the wildfire in British Columbia occurs in the summer period.

2.2. Data set

The satellite data used in this study are Aqua/MODIS data covering the summer period (June to August) from 2003 to 2012. During the daytime, Aqua satellite overpass occurs at about 13:00 pm local time. Three MODIS land products (collection V005), the daily 1 km land surface temperature product (MYD11A1), daily 500 m land surface reflectance product (MYD09GA), and 16-day 1 km albedo product (MCD43B3), were collected from USGS Land Processes Distributed Active Archive Center (LP DAAC). MYD11A1 provides daytime and night-time LST, which is derived from two thermal infrared bands using a generalized split-window algorithm (Wan 1999). MYD09GA provides land surface reflectance from seven spectral bands (red, NIR₁, blue, green, NIR₂, SWIR₁, SWIR₂), which are atmospherically corrected using MODIS atmospheric products (Vermote and Vermeulen 1999). MCD43B3 provides land surface albedo, which is calculated based on a semi-empirical, kernel-driven bidirectional reflectance distribution function (BRDF) model (Strahler and Muller 1999). In addition, the 90 m Shuttle Radar Topography Mission (SRTM) digital elevation model (DEM) data of the study area were acquired from the US Geological Survey (USGS).

Air temperature data were collected from 288 weather stations in British Columbia operated by Environment Canada (Figure 1). Daily maximum temperatures at these stations from June to August 2003–2012 were used in this study. The quality control (QC) information in the MODIS LST product provides the quality level of each pixel, including cloud mask flag. Based on the cloud mask derived from the QC of the MODIS LST product, T_a measurements under cloudy conditions were removed, leaving 62,746 samples for model development and validation.

3. Methodology

3.1. Variable selection

Near-surface air temperature is driven more by land surface temperature than by direct solar radiation (Zakšek and Schroedter-Homscheidt 2009), making LST an important variable for estimating T_a . Other parameters, such as vegetation cover, soil moisture, solar radiation, and albedo also have some influence on air temperature. In previous

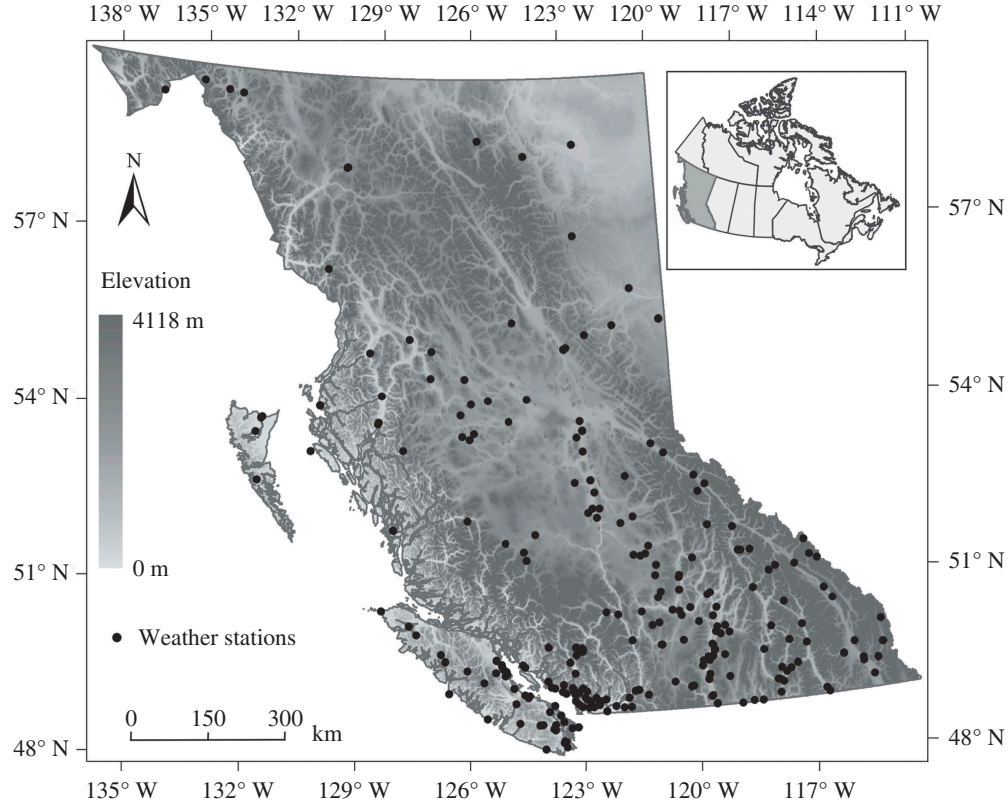


Figure 1. Elevation map of the study area and the distribution of weather stations.

studies, several variables were employed to estimate air temperature. For example, the variables used by Benali et al. (2012) included LST, Julian Day, elevation, and distance to coast. The variables used by Kim and Han (2013) included LST, NDVI, altitude, and solar zenith angle. The variables used by Cristóbal, Ninyerola, and Pons (2008) included LST, NDVI, and albedo. The variables used by Zakšek and Schroedter-Homscheidt (2009) included LST, NDVI, solar zenith, albedo, solar radiation, and altitude. After comprehensive consideration of these variables, nine variables were selected as the predictors for modelling air temperature: daytime LST, NDVI, modified normalized difference water index (MNDWI), latitude, longitude, distance to ocean, altitude, albedo, and solar radiation.

Daytime LST was extracted from the MYD11A1 product. Land surface reflectance of green, red, NIR₁, and SWIR bands was extracted from the MYD09GA product to calculate NDVI and MNDWI, which were then resampled to 1 km resolution. Surface shortwave (0.3–5.0 μm) broadband albedo was extracted from the MCD43B3 product. Distance to the ocean was calculated based on the western coastline of North America. Altitude data were acquired from the SRTM DEM data and resampled to 1 km resolution to be consistent with MODIS data. Daily solar radiation was calculated based on the Julian Day, latitude, slope, and aspect derived from altitude data.

NDVI is calculated using the following equation (Tucker 1979):

$$\text{NDVI} = \frac{\rho_{\text{NIR}} - \rho_{\text{red}}}{\rho_{\text{NIR}} + \rho_{\text{red}}}, \quad (1)$$

where ρ_{NIR} and ρ_{red} are the reflectance of NIR and red bands, respectively.

MNDWI is calculated using the following equation (Xu 2006):

$$\text{MNDWI} = \frac{\rho_{\text{green}} - \rho_{\text{SWIR}}}{\rho_{\text{green}} + \rho_{\text{SWIR}}}, \quad (2)$$

where ρ_{green} and ρ_{SWIR} are the reflectance of green and SWIR bands, respectively.

3.2. Model selection

Using the nine variables as predictors, two different methods were employed to estimate daily maximum T_a in British Columbia: linear regression and random forest. Linear regression is the most popular statistical model for estimating air temperature and requires assumptions of normality of residuals, constant variance, and true linearity of the modelled relationship (Helsel and Hirsch 1992). Random forest is a nonparametric statistical method proposed by Breiman (2001). Unlike traditional statistical methods that assume a parametric model for prediction, random forest is an ensemble learning technique based on a collection of tree predictors. It consists of a combination of many decision trees, where each tree is built using a deterministic algorithm by a bootstrap sample, leaving the remaining data points for validation. A decision tree is generated from a random subset of the training data and the nodes are split using the best split predictor among a subset of randomly selected variables. Predictions produced by the random forest model are the average of the results of all the individual trees that make up the ‘forest’. Compared with statistical analysis methods, random forest has the advantages of making no distributional assumptions about the predictors, measuring variable importance, and being less sensitive to noise or overfitting (Armitage and Ober 2010; Breiman 2001; Ismail and Mutanga 2010). In recent years, random forest has increasingly been applied in remote-sensing studies, most of which were focused on land cover classification (Chan and Paelinckx 2008; Ghimire, Rogan, and Miller 2010; Guo et al. 2011; Pal 2005; Timm and Mcgarigal 2012).

Linear regression was performed in the R statistical software. A stepwise multiple linear regression analysis was conducted to identify the best set of variables, with the Akaike Information Criterion (AIC) as selection criterion. Results reveal that the linear regression equation including all nine variables achieves the lowest AIC value. Therefore, all nine variables were employed to generate linear regression equation. The random forest model was also implemented in the R statistical software, using the ‘randomForest’ package (Liaw and Wiener 2002). All nine variables were also included in the random forest model. To run the random forest model, two important parameters should be defined: the number of trees to grow (ntree) and the number of variables to use at each node (mtry). These two parameters were optimized based on the percentage variance explained by the model. The mtry value was tested from 1 to 9 with a single interval, and the ntree value was tested using the following six values: 50, 100, 200, 500, 1000, and 2000. Figure 2 shows the variations in percentage variance explained with different ntree and mtry values. The highest values are achieved at mtry = 3 and high ntree values (ntree = 1000 or 2000). Considering that higher ntree values require higher computational cost, the ntree value was set to 1000 and the mtry value to 3 to run the random forest model.

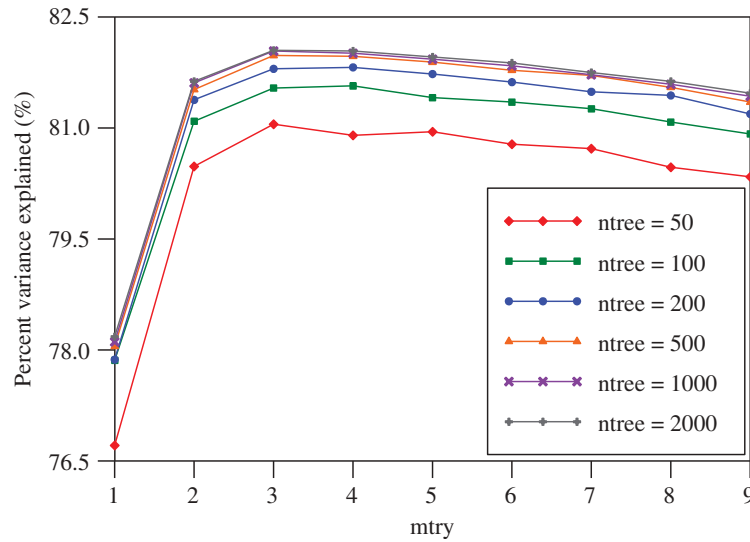


Figure 2. Variation in percentage variance explained by the random forest model with different ntree and mtry values.

The relationship between observed T_a and remotely sensed LST is not limited to a single pixel, because the temperature of the near-surface air mass in a given area is influenced by energy exchanges with the land surface over a larger upwind area. This is especially important in complex terrain where LST can vary over short distances due to insolation and altitude changes. Previous studies confirm this by showing that higher correlation coefficients were found between T_a and spatially averaged LST than those between T_a and single-pixel LST (Kawashima et al. 2000; Nichol and Wong 2008; Xu, Qin, and Shen 2012). To determine the proper spatial window size for estimating air temperature, the mean LST of 1×1 , 3×3 , 5×5 , 7×7 , 9×9 , 11×11 , 13×13 , and 15×15 km windows around weather stations was calculated. Figure 3 shows the variations in correlation coefficient between T_a and LST with the window size used for

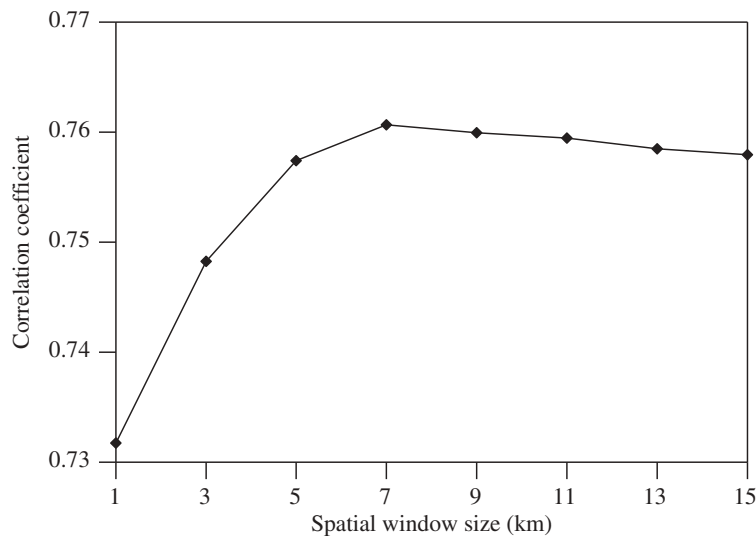


Figure 3. Variation of the correlation coefficient between T_a and LST with the window size used to spatially average the LST data.

averaging LST. It can be seen that the correlation coefficient initially increases rapidly with increasing window size and reaches its maximum value at the $7 \text{ km} \times 7 \text{ km}$ window size, after which it decreases slowly with increasing window size. Based on this result, the $7 \text{ km} \times 7 \text{ km}$ window size was selected for spatial averaging of all satellite-derived data layers prior to model development.

3.3. Model validation

The performance of the two models was assessed using cross-validation with the 62,746 samples from 288 weather stations. All samples from each station were used in turn as the validation data set to test the model, while the remaining samples were used as the training data set to fit the model. This process was repeated until all stations' samples had been used once as validation data. Mean absolute error (MAE) and coefficient of determination (R^2) were calculated from the measured and estimated T_a values to assess model performance.

The importance of predictors in each model, defined as the impact on the model accuracy when the variable was removed (Briand, Freimut, and Vollei 2004; Jeong et al. 2010), was also assessed. At a time, one of these nine variables was removed and the remaining eight variables used to run the model. The increase of estimation error caused by the removal of the variable, measured by the percentage increase in MAE (%IncMAE), was used to assess the importance of the variable removed. Variables with larger %IncMAE values were considered more important for estimating T_a .

4. Results and discussion

4.1. Model performance

Spatially averaged values of LST, NDVI, MNDWI, latitude, longitude, distance to ocean, altitude, albedo, and solar radiation were calculated and used as predictors of T_a in linear regression and random forest models. Equation (3) gives the linear regression equation for estimating T_a . Note that the structure of the random forest model, which is nonparametric, cannot be similarly provided.

$$\begin{aligned} T_{a_max} = & 0.6776 \text{ LST} + 8.62 \text{ NDVI} - 0.2976 \text{ MNDWI} + 0.1146 \text{ Lat} \\ & + 0.1446 \text{ Lon} + 0.0029 \text{ Dis} - 0.0012 \text{ H} - 35.5791 \text{ Al} \\ & - 0.0676 \text{ } W_s + 29.3955, \end{aligned} \quad (3)$$

where T_{a_max} is the daily maximum T_a ($^{\circ}\text{C}$), LST is the land surface temperature ($^{\circ}\text{C}$), Lat is the latitude, Lon is the longitude, Dis is the distance to the ocean (km), H is the altitude angle (m), Al is the surface albedo, and W_s is the solar radiation (M J m^{-2}).

Figure 4 shows the scatter plots between measured and estimated T_a from the linear regression model (left) and the random forest model (right). The linear regression model produces an MAE of 2.41°C and R^2 of 0.64, and the random forest model produces a higher accuracy with an MAE of 2.02°C and R^2 of 0.74. In addition, the scatter of the random forest model is considerably closer to the 1:1 line than that of the linear regression model. The comparison between the results obtained with the random forest model and the linear regression model shows that random forest has much higher estimation accuracy. This may be attributed partly to the complex terrain of the study area.

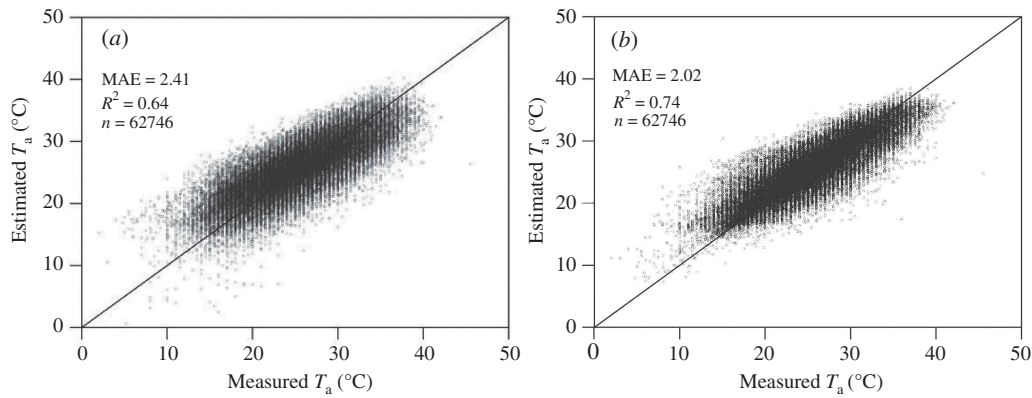


Figure 4. Scatter plot between measured and estimated daily maximum T_a from the linear regression model (a) and random forest model (b).

Differences in topography, land surface properties, and solar radiation lead to different land surface–atmosphere interactions. As a single global model, linear regression cannot properly handle the complicated relationships between T_a and environmental variables at different conditions. Additionally, the relationship between T_a and some variables in heterogeneous landscapes cannot be assumed to be linear, in which case the linear regression model will perform poorly. By contrast, random forest is able to effectively model non-linear and complex relationships by constructing a multitude of decision trees, and therefore works well in mountainous areas.

The distribution of residuals, the difference between measured T_a and estimated T_a from the random forest model at 7×7 pixel size, was also examined (Figure 5). The mean value of residuals is 0.09°C , suggesting that the model is very slightly overestimating T_a . About 33.04% of the estimated T_a falls within $\pm 1^\circ\text{C}$ of the observed T_a , 77.25% falls

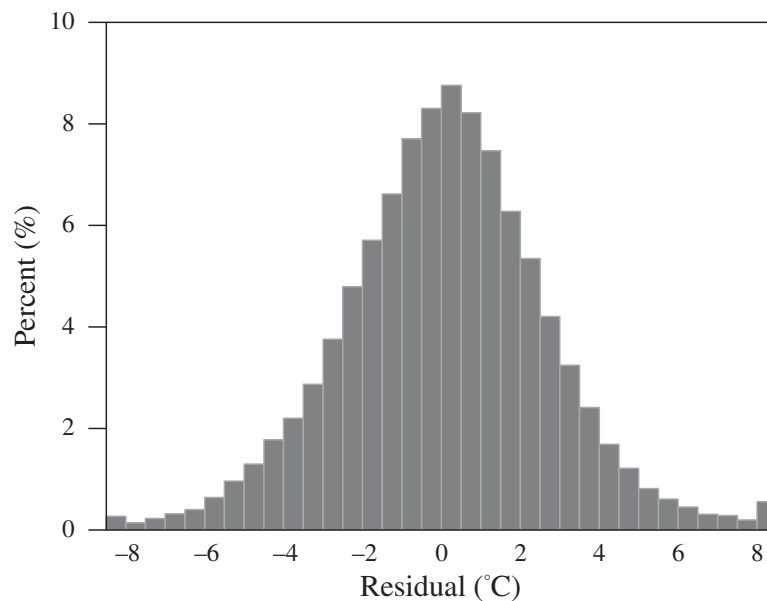


Figure 5. Histogram of residuals of the random forest model.

Table 1. Importance of variables in random forest model.

Variable	%IncMAE (%)
LST	106.43
NDVI	25.80
MNDWI	26.93
Altitude	7.90
Distance to sea	7.53
Latitude	7.94
Longitude	7.67
Albedo	21.64
Solar radiation	29.29

within $\pm 3^{\circ}\text{C}$, and 93.89% falls within $\pm 5^{\circ}\text{C}$. The estimated T_a shows good overall agreement with the measured T_a . Taking into account the complex terrain and large area of the study area, these results are satisfactory.

Table 1 shows the importance of variables in terms of the percentage increase in MAE, which represents the influence on the random forest model when each variable is removed. Higher %IncMAE indicates greater variable importance. LST has the highest importance (%IncMAE = 106.43%), with MAE more than doubling when it is removed from model training. This indicates that LST is the most important variable in the model, which can be attributed to the fact that near-surface atmosphere is directly heated by the land surface. Solar radiation shows the second highest importance (%IncMAE = 29.29%), which is also a considerable source of heat for the atmosphere. MNDWI, NDVI, and albedo, which effectively represent the land surface characteristics such as soil moisture, vegetation cover, and reflection ability, also show relative high importance (%IncMAE = 26.93%, 25.80%, and 21.64%, respectively). However, other environmental variables (latitude, longitude, altitude, and distance to sea) have low importance (%IncMAE = 7.94%, 7.67%, 7.90%, and 7.53%, respectively). The lower importance of these four temporally stable geographical variables may be attributed to the fact that remotely sensed variables can effectively describe both spatial and temporal variations in environmental properties, while geographical variables can only describe spatial variation.

4.2. Spatial variation of T_a

Figure 6 shows the average daily maximum T_a map of British Columbia in the summer periods from 2003 to 2012, as predicted by the random forest model. The area exhibits substantial spatial variation in air temperature, which is most strongly influenced by altitude, latitude, terrain, and distance to the ocean. Generally, the interior is hotter than the coastal areas, and the south is hotter than the north. The summer maximum T_a in most regions was found within the range $15\text{--}25^{\circ}\text{C}$, although the valleys located in the southern interior show higher temperatures ($>27^{\circ}\text{C}$) and the high-altitude areas of the Coast Mountains show lower temperatures ($<12^{\circ}\text{C}$). The Queen Charlotte Islands, Rocky Mountains, and the northern plateau also show relatively low temperatures.

Ten-year (2003–2012) averaged daily maximum T_a maps of each summer month are presented in Figure 7. Overall, the spatial distribution of T_a is similar among the three months although temperatures were lower in June than in July and August, which were very similar except in the northeastern plains and northern plateau where July is substantially hotter than August.

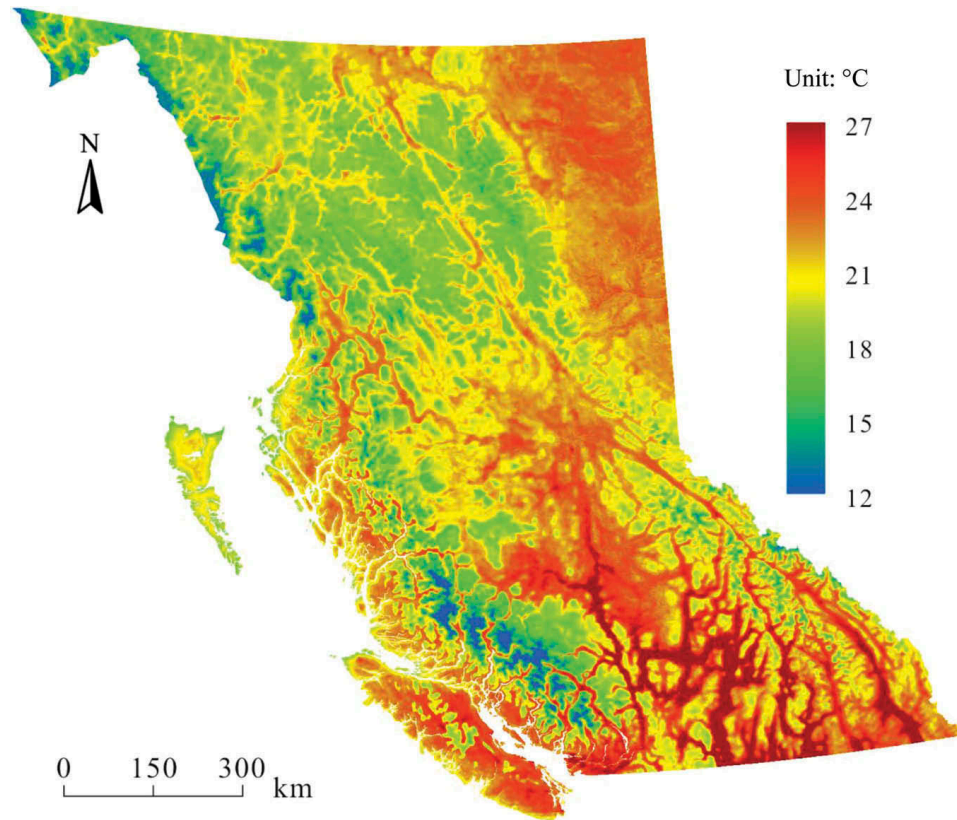


Figure 6. Spatial distribution of averaged daily maximum T_a for British Columbia in the summer periods from 2003 to 2012.

5. Conclusions

In this paper, the daily maximum air temperature in summer periods from 2003 to 2012 was estimated for British Columbia, Canada using 1 km Aqua/MODIS data. The correlation coefficient between observed T_a and remotely sensed LST shows an increasing trend, with spatial window size increasing from 1 km \times 1 km to 7 km \times 7 km, and subsequently decreasing slightly at window sizes larger than 7 km \times 7 km. This window size was therefore used to spatially average nine satellite-derived environmental variables, which were used as predictors of T_a in linear regression and random forest models. Cross-validation results show that the random forest model (MAE = 2.02°C, R^2 = 0.74) outperforms the linear regression model (MAE = 2.41°C, R^2 = 0.64). The distribution of residuals from the random forest model suggests that this method slightly overestimates T_a , with a mean residual value of 0.09°C. Most of the estimated T_a values were within the accuracy of 1–3°C (33.04% within 1°C and 77.25% within 3°C). The satisfactory results suggest that random forest models at proper spatial size can effectively estimate T_a over complex terrain regions. Additionally, variable importance analysis indicates that LST is the most important variable for T_a estimation and remotely sensed variables contribute more than geographical variables.

Based on the estimated T_a from the random forest model, the spatial variation of summer daily maximum T_a in British Columbia was studied. Maximum T_a exhibits a significant regional variability in the study area, which is highly influenced by altitude, terrain, distance to ocean, and other environmental variables. Temperature in June is lower than that in July and August. Most regions show similar temperature in July and August,

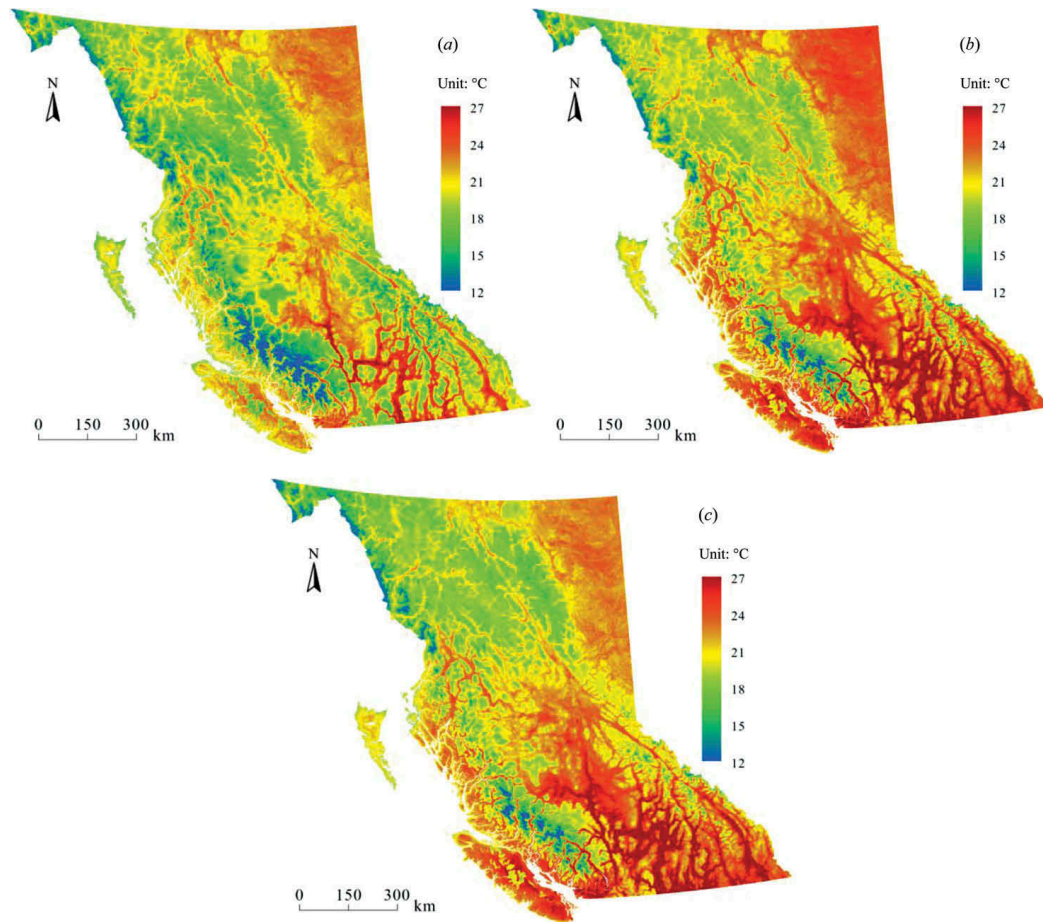


Figure 7. Spatial distributions of averaged daily maximum T_a of British Columbia for June (a), July (b), and August (c) from 2003 to 2012.

except for the northeastern plains and northern plateau. With the use of satellite remote sensing, spatially detailed information on air temperature in large and mountainous areas can be obtained, which is of great significance for understanding wildfire risk, forest distribution, and growth.

Acknowledgements

The authors would like to thank the Land Processes Distributed Active Archive Center for providing Moderate Resolution Imaging Spectroradiometer (MODIS) data, US Geological Survey for providing Shuttle Radar Topography Mission (SRTM) digital elevation model (DEM) data, and Environment Canada for providing meteorological data. We also thank Dr Meg Krawchuk of Simon Fraser University for her valuable suggestions. The authors would like to thank the two reviewers for their valuable comments and suggestions to improve this paper.

Funding

This research is financially supported by the National Natural Science Foundation of China [41201369], the Major State Basic Research Development Programme of China [2011CB952002, 2010CB950701], the Pacific Institute for Climate Solutions, and the Urban Meteorological Research Foundation of Beijing Urban Meteorological Research Institute [IUMKY&UMRF201102].

References

- Aldersley, A., S. J. Murray, and S. E. Cornell. 2011. "Global and Regional Analysis of Climate and Human Drivers of Wildfire." *Science of the Total Environment* 409: 3472–3481. doi:10.1016/j.scitotenv.2011.05.032.
- Armitage, D., and H. K. Ober. 2010. "A Comparison of Supervised Learning Techniques in the Classification of Bat Echolocation Calls." *Ecological Informatics* 5: 465–473. doi:10.1016/j.ecoinf.2010.08.001.
- B.C. Ministry of Forests, Mines and Lands. 2010. *The State of British Columbia's Forests*. 3rd ed. Victoria: Forest Practices and Investment Branch. Accessed April 15, 2013. http://www.for.gov.bc.ca/hfp/sof/2010/SOF_2010_Web.pdf
- Benali, A., A. C. Carvalho, J. P. Nunes, N. Carvalhais, and A. Santos. 2012. "Estimating Air Surface Temperature in Portugal Using MODIS LST Data." *Remote Sensing of Environment* 124: 108–121. doi:10.1016/j.rse.2012.04.024.
- Benavides, R., F. Montes, A. Rubio, and K. Osoro. 2007. "Geostatistical Modelling of Air Temperature in a Mountainous Region of Northern Spain." *Agricultural and Forest Meteorology* 146: 173–188. doi:10.1016/j.agrformet.2007.05.014.
- Breiman, L. 2001. "Random Forests." *Machine Learning* 45: 5–32. doi:10.1023/A:1010933404324.
- Briand, L. C., B. Freimut, and F. Vollei. 2004. "Using Multiple Adaptive Regression Splines to Support Decision Making in Code Inspections." *Journal of Systems and Software* 73: 205–217. doi:10.1016/j.jss.2004.01.015.
- Carrega, P. 1995. "A Method for the Reconstruction of Mountain Air Temperatures with Automatic Cartographic Applications." *Theoretical and Applied Climatology* 52: 69–84. doi:10.1007/BF00865508.
- Chan, J. C.-W., and D. Paelinckx. 2008. "Evaluation of Random Forest and Adaboost Tree-Based Ensemble Classification and Spectral Band Selection for Ecotope Mapping Using Airborne Hyperspectral Imagery." *Remote Sensing of Environment* 112: 2999–3011. doi:10.1016/j.rse.2008.02.011.
- Cristóbal, J., M. Ninyerola, and X. Pons. 2008. "Modeling Air Temperature through a Combination of Remote Sensing and GIS Data." *Journal of Geophysical Research* 113: D13106. doi:10.1029/2007JD009318.
- Czajkowski, K. P., T. Mulhern, S. N. Goward, J. Cihlar, R. O. Dubayah, and S. D. Prince. 1997. "Biospheric Environmental Monitoring at BOREAS with AVHRR Observations." *Journal of Geophysical Research* 102: 29651–29662. doi:10.1029/97JD01327.
- Dodson, R., and D. Marks. 1997. "Daily Air Temperature Interpolated at High Spatial Resolution over a Large Mountainous Region." *Climate Research* 8: 1–20. doi:10.3354/cr008001.
- Duhan, D., A. Pandey, K. P. S. Gahalaut, and R. P. Pandey. 2013. "Spatial and Temporal Variability in Maximum, Minimum and Mean Air Temperatures at Madhya Pradesh in Central India." *Comptes Rendus Geoscience* 345: 3–21. doi:10.1016/j.crte.2012.10.016.
- Florio, E. N., S. R. Lele, Y. C. Chang, R. Sterner, and G. E. Glass. 2004. "Integrating AVHRR Satellite Data and NOAA Ground Observations to Predict Surface Air Temperature: A Statistical Approach." *International Journal of Remote Sensing* 25: 2979–2994. doi:10.1080/01431160310001624593.
- Ghimire, B., J. Rogan, and J. Miller. 2010. "Contextual Land-Cover Classification: Incorporating Spatial Dependence in Land-Cover Classification Models Using Random Forests and the Getis Statistic." *Remote Sensing Letters* 1: 45–54. doi:10.1080/01431160903252327.
- Goward, S. N., R. H. Waring, D. G. Dye, and J. L. Yang. 1994. "Ecological Remote-Sensing at OTTER: Satellite Macroscale Observations." *Ecological Applications* 4: 322–343. doi:10.2307/1941937.
- Guo, L., N. Chehata, C. Mallet, and S. Boukir. 2011. "Relevance of Airborne Lidar and Multispectral Image Data for Urban Scene Classification Using Random Forests." *ISPRS Journal of Photogrammetry and Remote Sensing* 66: 56–66. doi:10.1016/j.isprsjprs.2010.08.007.
- Helsel, D. R., and R. M. Hirsch. 1992. *Statistical Methods in Water Resources*, 296–299. Amsterdam: Elsevier.
- Holden, Z. A., M. A. Crimmins, S. A. Cushman, and J. S. Littell. 2011. "Empirical Modeling of Spatial and Temporal Variation in Warm Season Nocturnal Air Temperatures in Two North Idaho Mountain Ranges, USA." *Agricultural and Forest Meteorology* 151: 261–269. doi:10.1016/j.agrformet.2010.10.006.

- Ismail, R., and O. Mutanga. 2010. "A Comparison of Regression Tree Ensembles: Predicting *Sirex noctilio* Induced Water Stress in *Pinus patula* Forests of Kwazulu-Natal, South Africa." *International Journal of Applied Earth Observation and Geoinformation* 12: S45–S51. doi:10.1016/j.jag.2009.09.004.
- Jang, J.-D., A. A. Viau, and F. Anctil. 2004. "Neural Network Estimation of Air Temperatures from AVHRR Data." *International Journal of Remote Sensing* 25: 4541–4554. doi:10.1080/01431160310001657533.
- Jeong, K., A. B. Kahng, B. Lin, and K. Samadi. 2010. "Accurate Machine-Learning-Based On-Chip Router Modeling." *IEEE Embedded Systems Letters* 2: 62–66. doi:10.1109/LES.2010.2051413.
- Kawashima, S., T. Ishida, M. Minomura, and T. Miwa. 2000. "Relations between Surface Temperature and Air Temperature on a Local Scale during Winter Nights." *Journal of Applied Meteorology* 39: 1570–1579. doi:10.1175/1520-0450(2000)039<1570:RBSTAA>2.0.CO;2.
- Kim, D., and K. Han. 2013. "Remotely Sensed Retrieval of Midday Air Temperature Considering Atmospheric and Surface Moisture Conditions." *International Journal of Remote Sensing* 34: 247–263. doi:10.1080/01431161.2012.712235.
- Kurtzman, D., and R. Kadmon. 1999. "Mapping of Temperature Variables in Israel: A Comparison of Different Interpolation Methods." *Climate Research* 13: 33–43. doi:10.3354/cr013033.
- Liaw, A., and M. Wiener. 2002. "Classification and Regression by Random Forest." *R News* 2: 18–22.
- Litschert, S. E., T. C. Brown, and D. M. Theobald. 2012. "Historic and Future Extent of Wildfires in the Southern Rockies Ecoregion, USA." *Forest Ecology and Management* 269: 124–133. doi:10.1016/j.foreco.2011.12.024.
- Nichol, J. E., and M. S. Wong. 2008. "Spatial Variability of Air Temperature and Appropriate Resolution for Satellite-Derived Air Temperature Estimation." *International Journal of Remote Sensing* 29: 7213–7223. doi:10.1080/01431160802192178.
- Nieto, H., I. Sandholt, I. Aguado, E. Chuvieco, and S. Stisen. 2011. "Air Temperature Estimation with MSG-SEVIRI Data: Calibration and Validation of the TVX Algorithm for the Iberian Peninsula." *Remote Sensing of Environment* 115: 107–116. doi:10.1016/j.rse.2010.08.010.
- Pal, M. 2005. "Random Forest Classifier for Remote Sensing Classification." *International Journal of Remote Sensing* 26: 217–222. doi:10.1080/01431160412331269698.
- Pape, R., and J. Löffler. 2004. "Modelling Spatio-Temporal Near-Surface Temperature Variation in High Mountain Landscapes." *Ecological Modelling* 178: 483–501. doi:10.1016/j.ecolmodel.2004.02.019.
- Pike, R. G., T. E. Redding, R. D. Moore, R. D. Winker, and K. D. Bladon, eds. 2010. *Compendium of Forest Hydrology and Geomorphology in British Columbia*. Victoria: B.C. Ministry of Forests and Range Forest Science Program; Kamloops: FORREX Forum for Research and Extension in Natural Resources. Accessed April 16, 2013. <http://www.for.gov.bc.ca/hfd/pubs/docs/lmh/Lmh66.htm>
- Prihodko, L., and S. N. Goward. 1997. "Estimation of Air Temperature from Remotely Sensed Surface Observations." *Remote Sensing of Environment* 60: 335–346. doi:10.1016/S0034-4257(96)00216-7.
- Rolland, C. 2003. "Spatial and Seasonal Variations of Air Temperature Lapse Rates in Alpine Regions." *Journal of Climate* 16: 1032–1046. doi:10.1175/1520-0442(2003)016<1032:SASVOA>2.0.CO;2.
- Stahl, K., R. D. Moore, J. A. Floyer, M. G. Asplin, and I. G. Mckendry. 2006. "Comparison of Approaches for Spatial Interpolation of Daily Air Temperature in a Large Region with Complex Topography and Highly Variable Station Density." *Agricultural and Forest Meteorology* 139: 224–236. doi:10.1016/j.agrformet.2006.07.004.
- Strahler, A. H., and J.-P. Muller. 1999. "MODIS BRDF/Albedo Product: Algorithm Theoretical Basis Document." Accessed May 8, 2013. http://modis.gsfc.nasa.gov/data/atbd/atbd_mod09.pdf
- Sun, Y.-J., J.-F. Wang, R.-H. Zhang, R. R. Gillies, Y. Xue, and Y.-C. Bo. 2005. "Air Temperature Retrieval from Remote Sensing Data Based on Thermodynamics." *Theoretical and Applied Climatology* 80: 37–48. doi:10.1007/s00704-004-0079-y.
- Timm, B. C., and K. Mcgarigal. 2012. "Fine-Scale Remotely-Sensed Cover Mapping of Coastal Dune and Salt Marsh Ecosystems at Cape Cod National Seashore Using Random Forests." *Remote Sensing of Environment* 127: 106–117. doi:10.1016/j.rse.2012.08.033.
- Tucker, C. J. 1979. "Red and Photographic Infrared Linear Combinations for Monitoring Vegetation." *Remote Sensing of Environment* 8: 127–150. doi:10.1016/0034-4257(79)90013-0.

- Vermote, E. F., and A. Vermeulen. 1999. "Atmospheric Correction Algorithm: Spectral Reflectances (MOD09). MODIS Algorithm Technical Background Document." Accessed May 10, 2013. http://modarch.gsfc.nasa.gov/data/atbd/atbd_mod08.pdf
- Vogt, J., A. A. Viau, and F. Paquet. 1997. "Mapping Regional Air Temperature Fields Using Satellite Derived Surface Skin Temperatures." *International Journal of Climatology* 17: 1559–1579. doi:10.1002/(SICI)1097-0088(19971130)17:14<1559::AID-JOC211>3.0.CO;2-5.
- Wan, Z. 1999. "MODIS Land-Surface Temperature. Algorithm Theoretical Basis Document." Accessed May 10, 2013. http://modis.gsfc.nasa.gov/data/atbd/atbd_mod11.pdf
- Wloczyk, C., E. Borg, R. Richter, and K. Miegel. 2011. "Estimation of Instantaneous Air Temperature above Vegetation and Soil Surfaces from Landsat 7 ETM+ Data in Northern Germany." *International Journal of Remote Sensing* 32: 9119–9136. doi:10.1080/01431161.2010.550332.
- Xu, H. 2006. "Modification of Normalised Difference Water Index (NDWI) to Enhance Open Water Features in Remotely Sensed Imagery." *International Journal of Remote Sensing* 27: 3025–3033. doi:10.1080/01431160600589179.
- Xu, Y., Z. Qin, and Y. Shen. 2012. "Study on the Estimation of Near Surface Air Temperature from MODIS Data by Statistical Methods." *International Journal of Remote Sensing* 33: 7629–7643. doi:10.1080/01431161.2012.701351.
- Zakšek, K., and M. Schroedter-Homscheidt. 2009. "Parameterization of Air Temperature in High Temporal and Spatial Resolution from a Combination of the SEVIRI and MODIS Instruments." *ISPRS Journal of Photogrammetry and Remote Sensing* 64: 414–421. doi:10.1016/j.isprsjprs.2009.02.006.
- Zhang, W., Y. Huang, Y. Yu, and W. Sun. 2011. "Empirical Models for Estimating Daily Maximum, Minimum and Mean Air Temperatures with MODIS Land Surface Temperatures." *International Journal of Remote Sensing* 32: 9415–9440. doi:10.1080/01431161.2011.560622.
- Zhu, W., A. Lü, and S. Jia. 2013. 'Estimation of Daily Maximum and Minimum Air Temperature Using MODIS Land Surface Temperature Products.' *Remote Sensing of Environment* 130: 62–73. doi:10.1016/j.rse.2012.10.034.